JOURNAL

OF

GEOMAGNETISM

AND

GEOELECTRICITY

VOL. II NO. 3

SOCIETY

OF

TERRESTRIAL MAGNETISM AND ELECTRICITY

Oct. 1950

KYOTO

Recent Progress in Palaeomagnetism in Japan

By N. KUMAGAI, N. KAWAI and T. NAGATA

Geological and Mineralogical Institute Kyoto University

Geophysical Institute Tokyo University

The scientific studies of determining the direction of geomagnetic field in the old geologic times from the data of the remanent magnetization of rocks have been continued by us since the pioneer work carried out by M. Matuyama in 1929.(1)

The specimens examined in our studies are the lava flows and the horizontal sedimentary layers of various localities of Japan. The rather intense magnetization of volcanic rocks were measured by astatic magnetometers both in Tokyo and Kyoto, while the weak magnetization of specimens of sedimentary layers were examined by the induction-type equipment(2) or by a magnetometer of special type(3) in Tokyo and by a resonance-type magnetometer newly designed(4) in Kyoto.

From each lava flow, specimen pieces of five to twenty in number were cut off, the direction of the pice *in situ* being measured. On the other hand, a large number of specimens were systematically taken in various different localities and depths of each layer.

The final results of measurements are summarized in Tables I and II, where the mean values of dip and the deviation of declination from its present value are shown together with the localities, petrological characters and ages of rocks.

As to the reliability of direction of remanent magnetization of volcanic lavas, the result shown in the upper part of Table II will give a significant proof. The ejection and solidification of these lavas were actually observed, and it was firmly ascertained that their thermo-remanent magnetism keeps the direction of geomagnetic field in their neighbourhood. Thus we may say that, so far as we select the large and unbroken lava, the direction of their remanent magnetization can indicate that of geomagnetic field at the time of their cooling.

As will be seen in Table I, the volcanic lavas and sedimentary layers ejected and deposited respectively during the geological times from Upper Neogene through Lower Holocene almost Keep the direction of their magnetisation nearly equal to the present value of geomagnetic force, except the Azuki-tuff (Upper Neogene deposits), the lava at volcano Sigi (Upper Neogene ejecta) and the dyke rock at Kasuga (Lower Holocene).

Table I. Geological Ages.

No.	Locality	Rock	Age	ΔD(E)	I	Observer
1	Kasuga (Nara)	Dolerite dyke	Lower Holocene	76°0±0°4	30°5±2°4	Kawai
2	Mikasa (Nara)	Two-pyroxene andesite	Lower Holocene	−1.1±1.8	36.9±3.8	Kawai
3	Kabuto (Hyōgo)	Bronzite andesite	Lower Holocene	−8.4±2.2	49.8±1.8	Kawai
4	Tiba	Narita-bed (fine sand layer)	Pleistocene	4.5	56.3	Nagata*
5	Yawatano (Amagi)	Two-pyroxene andesite	Pleistocene	12.7±1.5	47.3±1.6	Nagata
6	Omuro	Olivine-basalt	Pleistocene	8.3±4.2	44.3±3.8	Nagata
7	Aziro	Olivine-augite basalt	Lower part of Pleistocene	−26.7±2.0	49.7±1.5	Nagata
8	Osaka	Azuki-tuff	Upper part of upper Neogene	−159.5±1.8	−126.3±6.3	Kawai
9	Sigi (Osaka, Nara)	Two-pyroxene andesite	Upper part of upper Neogene	−168.4±4.6	−136.8±10.8	Kawai
10	Odake (Nara)	Sanukitic andesite	Lower part of upper Neogene	−13.5±1.7	25.5±6.3	Kawai
11	Nizyo 1. (Nara)	Bronzite andesite	Lower part of upper Neogene	9.3±2.6	54.3±1.9	Kawai
12	Nizyo 2. (Nara)	Biotite-hornblende andesite	Lower part of upper Neogene	−8.8±5.3	60.6±6.9	Kawai
13	Myōzon (Nara)	Hornblend Hyper-sthen andesite	Lower part of upper Neogene	−8.9±2.4	54.3±2.2	Kawai
14	Unebi (Nara)	Biotite andesite	Lower part of upper Neogene	−9.8±1.9	45.3±2.1	Kawai
15	Miminasi (Nara)	Biotite andesite	Lower part of upper Neogene	−7.0±3.4	51.2±2.7	Kawai
16	Sidara (Aiti)	Basaltic andesite	Miocene	28.3±2.9	65.7±8.8	Sannodo & Magata

* The average value of 271 samples collected from the whole parts of layer of 7 m in thickness.

Table II. Present and Historical Ages.

No.	Locality	Rock	Age	ΔD(E)	I	Observer
17	Mihara (Oosima)	Basalt	1914	−0°3±0°7	49°0±0°9	Nagata
18	Mihara (Oosima)	Basalt	1940	−0.0±0.7	48.4±0.6	Nagata
19	Miyake-zima	Olivine-pyroxene basalt	1940	−0.1±0.5	48.2±0.4	Nagata
20	Aokigahara (Huzi)	Basalt	864	−7.9±0.9	43.3±0.6	Nagata
21	An'ei lava (Mihara)	Basalt	1778	6.4±1.9	44.3±1.6	Nagata

Fig. 1 a.

Lower hemisphere

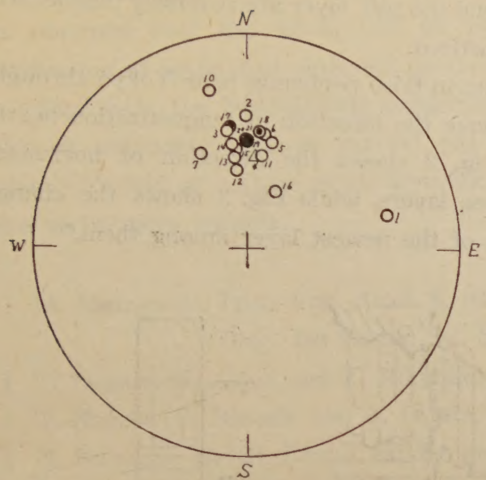

North seeking polarizations

- △ Sedimentary rock
- ○ Geological age volcanic rocks
- ◉ Historical age volcanic rocks
- ● Present volcanic rocks

Fig. 1 b.

Lower hemisphere

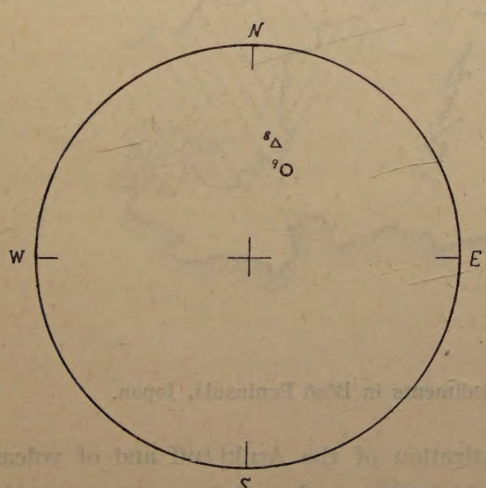

South seeking polarizations

- △ Sedimentary rock
- ○ Volcanic rock

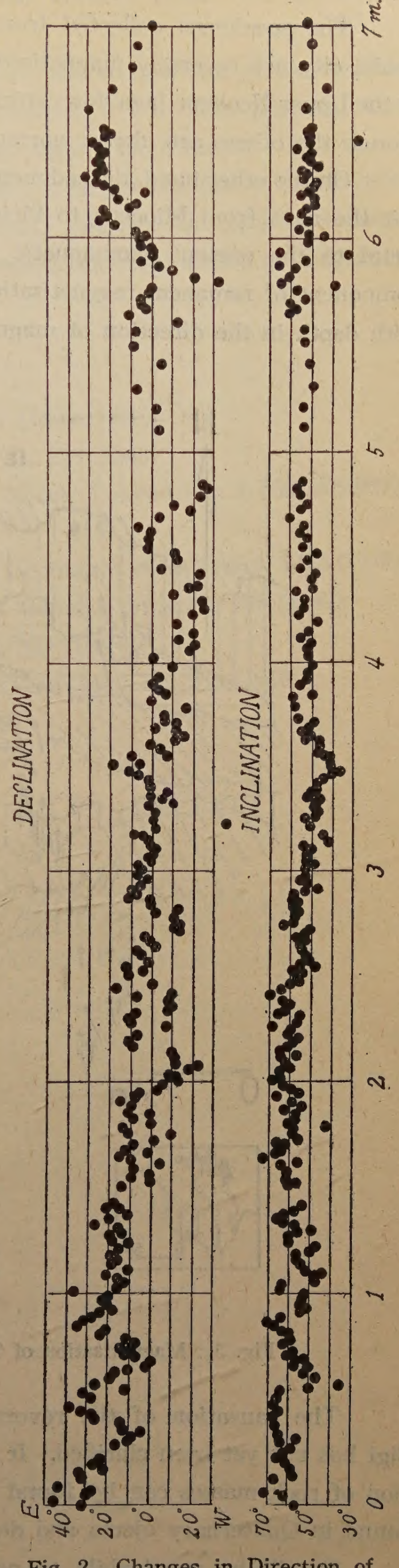

Fig. 2. Changes in Direction of Remanent Magnetization of Narita-bed with Depth.

The specimens collected from various localities in the Azuki-tuff layer around Osaka city are reversely magnetized, while the lava specimens from volcano Sigi, one of the Upper Neogene lava flows situated around the tuff layer are reversely magnetized, though the others are almost normally magnetized.

On the other hand, the sedimentary layers in Bōsō peninsula near Tokyo throughout the ages from Miocene to Pleistocene have the direction of magnetization nearly equal to the present geomagnetic force. Fig. 2 shows the direction of horizontal component of remanent magnetization of these layers, while Fig. 3 shows the change with depth in the direction of magnetization of the newest layer among them.[5]

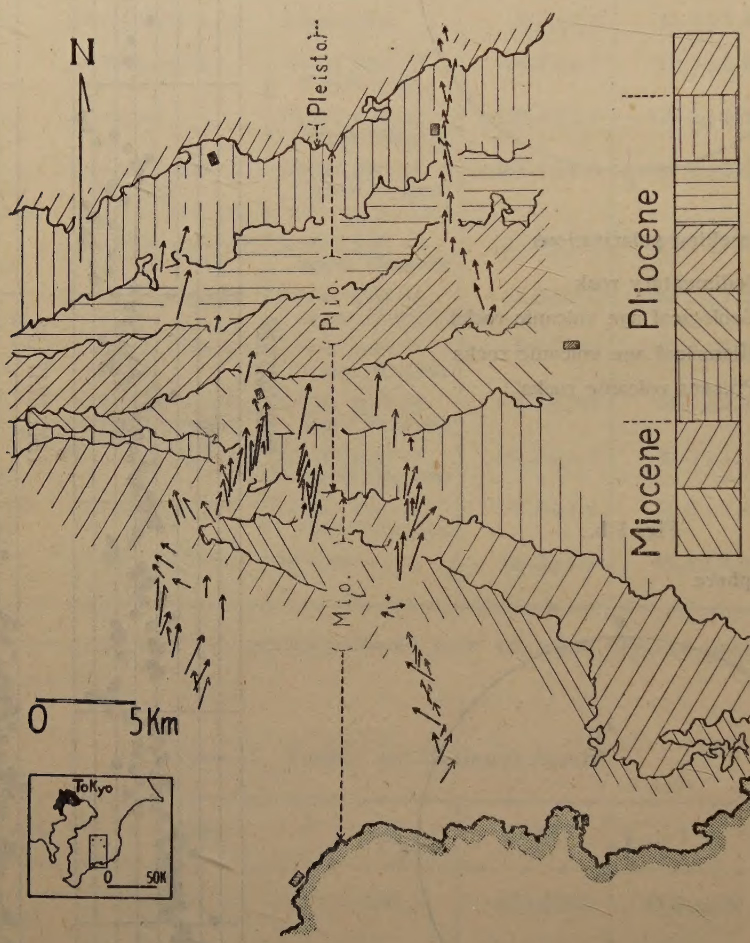

Fig. 3. Magnetization of Tertiary Sediments in Bôsô Peninsula, Japan.

The causation of the reverse magnetization of the Azuki-tuff and of volcano Sigi has not yet been clarified. It can be said, however, that the reverse magnetization of rock masses can be found only in Tertiary ejecta and deposits, and hardly found in Quaternary ejecta and deposits, so far concerning Japanese data.

It will be worthwhile to note that the data of reverse magnetization hitherto

found in England[6] and in Japan[1] are concerning the Tertiary ejecta and intrusions respectively.

In order to promote palaeomagnetism in future, the comparison of the similar data obtained over the world will be most fundamental. For this purpose, the identification of geological ages will become the most significant element.

Especially, the international cooperation in the systematic studies of horizontal strata of sediments such as carried out by McNish, Johnson, Murphy, Torreson, Graham[7,8,9] and us will be much desirable, since geological identification of sediments seems to be more reliable.

[1] M. Matuyama, Proc. Imp. Acad. **5**, 203 (1929).
Proc. 4th Pacific Sci. Cong., 567 (Jawa 1929).
[2] T. Nagata, K. Akasi and T. Rikitake, B.E.R.I., **21**, 276 (1943).
[3] T. Nagata, Y. Harada and A. Okada, Geophy. Notes, Tokyo Univ. **1**, No. 13 (1947).
[4] N. Kumagai and N. Kawai. (under press)
[5] T. Nagata, K. Hirao and H. Yoshikawa, Jour. Geomag. Geoel. Japan. **1**, 52 (1949).
[6] F.G. Bruckshaw and E.I. Robertson, M.N.R.A.S. Geophs. Suppl. **5**, 308 (1949).
[7] A.G. McNish and E.A. Johnson, Terr. Mag. **43**, 393 (1938).
[8] E.A. Johnson, T. Murphy and O.W. Torreson, Terr. Mag. **53**, 349 (1948).
[9] J.W. Graham, Jour. Geophys. Res. **54**, 131 (1949).

On the Diurnal Variation of Cosmic Rays: Part II
Annual Change of the Cosmic-Ray Diurnal Variation

By Yataro SEKIDO and Sekiko YOSHIDA

Physical Institute, Nagoya University

Duperier and Hogg have studied on the annual change of the cosmic-ray diurnal variation. Duperier[1] tried to explain the annual change, observed at one station (London), assuming a regular emission from the sun and a siderial time variation of cosmic-rays. Hogg[2] looked upon this as a seasonal change of the solar time variation, after his comparison of two sets of data obtained in each of the both hemisphere (London, Canberra). In this paper, similar treatment was done on the two other sets of data (Tokyo, Capetown), to get more appropriate construction on the annual change of the cosmic-ray diurnal variation, after the comparison of four sets of data, two in northern and two in southern hemisphere respectively.

Data used for this analysis are as follows (Table 1).

Table 1.

	Station			Observer	Duration
(Cp)	Capetown	34.0 S	18.5 E	Schonland[3]	Feb. 1933 — Jan. 1936
(Cn)	Canberra	35.3 S	149. E	Hogg	Sept. 1935 — Aug. 1940
(L)	London	51.5 N	0.	Duperier[1]	May. 1941 — Apr. 1944
(T)	Tokyo	35.7 N	139.7 E	S.R.I.*	July 1947 — June 1949

* Nishina Laboratory, Scientific Research Institute.

As the measure of the diurnal variation to be compared each other, 1st harmonics of the solar time variation of primary (i.e. barometer and temperature corrected) cosmic-ray intensities averaged in three months (Feb.–Apr., May–July, etc.) were computed. Temperature correction for the data obtained at Tokyo was done with the mean temperature of upper atmosphere observed at Tokyo or Tateno averaged in each month respectively. For we have had no meteorological data, at hand, corresponding to the observation at Capetown, the seasonal change of the diurnal variation of the temperature of the upper atmosphere at Tokyo and Tateno was computed, to use as a substitute for this purpose. 1st harmonics thus obtained are plotted in Fig. 1 as a harmonic dial refered to the local time of each station.

Concerning to each station respectively, consider the 1st harmonic vector of the diurnal variation D=M+Y, where M is the averaged vector characteristic to the station, and Y is the vector showing the annual change at the station. Then, M's are largely different among the stations, presumably due to the difference of the latitude, altitude, and type of instrument, and to the secular change of diurnal variation; while

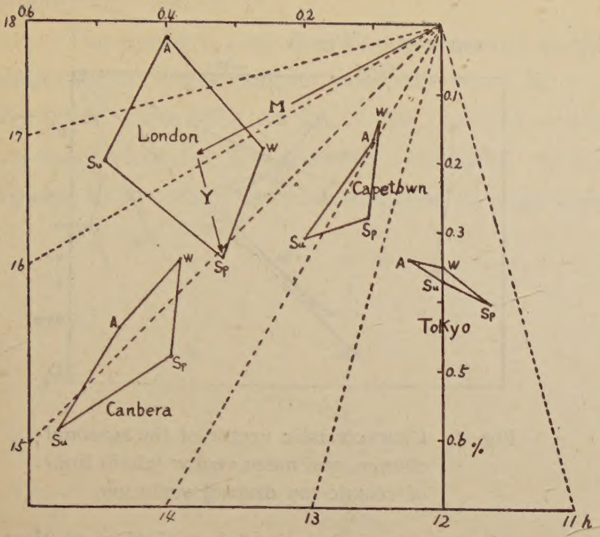

Fig. 1. Cosmic-ray diurnal variation observed at each of four stations.

Y's bear greater similarity, on which comparison will be done as follows.

Fig. 2 shows averages of Y's over four stations in different manners. (A) are seasonal means as the spring (Sp), the summer (Su), etc. (B) are means in the period containing the equinox (e) or solstices (s) respectively. (C) are means in Feb.–Apr. (3), May–July (6), etc. The radius of circle around each of these averaged vectors is equal to the standard deviation of the individual points used for that average. In the case of (A) and (B), the differences among the averaged vectors are larger than the radii of circles, or the dispersion of data. Both of (A) and (C) are annual change. Among them, (A) represents a change having opposite phase in the two hemisphere, or the seasonal change; while (C) represents the world-wide change. Now, assuming the world-wide change (C) attains the same value at every station as that represented by Fig. 2 (C), Y–C or the seasonal variation alone was taken out for each station, thus obtaining Fig. 3 (Y–C).

The dispersions of data corresponding to individual station (Cp, Cn, L, T) around the averaged seasonal variation (Sp, Su, A, W) are smaller than the case of Fig. 2 (A), and yet they have some regularities left. If the points attaching to A, W and Sp are rotated by 1, 2, and 3 rectangles respectively, thus obtaining Fig. 4 i(Y–C), then these points make groups for every station. This fact will mean that there are the vectors (Cp, Cn, L, T) characteristic to each station respectively, which rotate by a rectangle

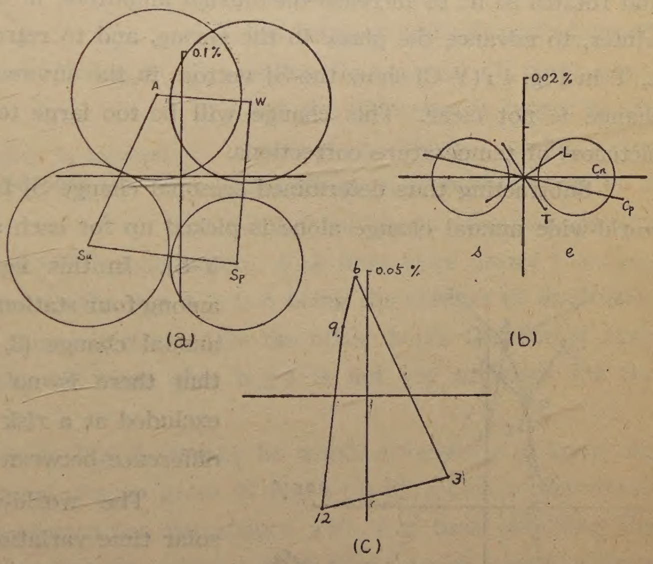

Fig. 2. Annual (a, c) and semi-annual (b) change of cosmic-ray diurnal variation.

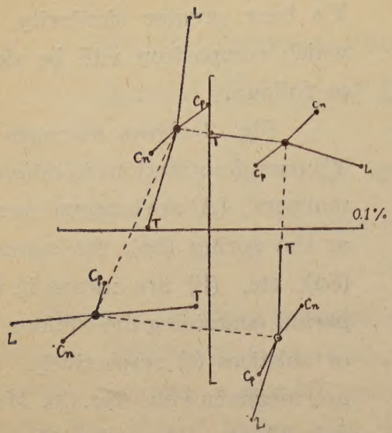

Fig. 3. Seasonal change of cosmic-ray diurnal variation.

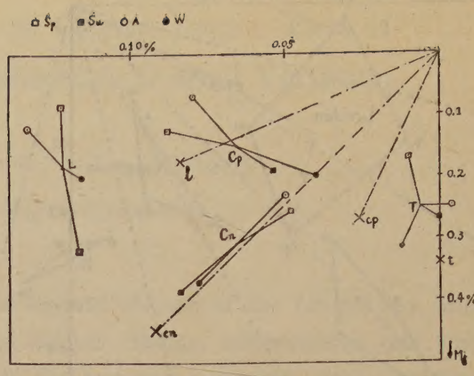

Fig. 4. Characteristic vector of the seasonal change, and mean vector (chain line) of cosmic-ray diurnal variation.

in each season, thus representing the seasonal change of the diurnal variation at that station. And, these four vectors are nearly proportional to the annual mean vectors Mj (j = Cp, Cn, L, T), Mj are reproduced in Fig. 4. In other words, the seasonal change of the cosmic-ray diurnal variation is represented by a characteristic vector Sj, which is nearly proportional to the annual mean vector of diurnal variation at that station and rotates so as to increase the diurnal amplitude in the summer, to decrease in the winter, to advance the phase in the spring, and to retrocedes in the autumn. Cp, Cn, L, T in Fig. 4 *i* (Y–C) show the Sj vectors in the summer. The cause of this seasonal change is not clear. This change will be too large to be explained with the incompleteness of temperature corrections.

Subtracting thus determined seasonal change Sj from the annual change Y, the world-wide annual change alone is picked up for each station and ploted in Fig. 5 as Y–Sj. In this figure, the dispersion of points among four stations is smaller than the averaged annual change (3, 6, 9, 12), and the hypothesis that there is no world-wide annual change is excluded at a risk smaller than 1%, though the difference between 6 and 9 is meaningless.

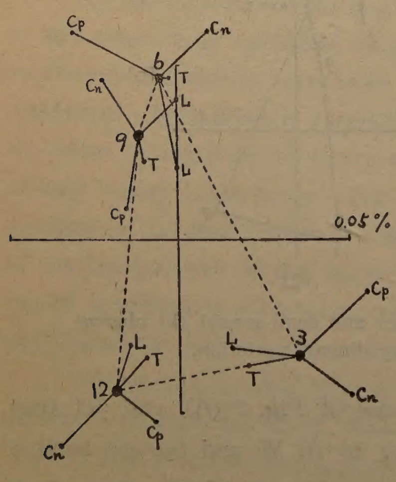

Fig. 5. World-wide annual change of cosmic-ray diurnal variation.

The world-wide annual change of the solar time variation thus obtained means that the cosmic-ray intensity increases by about 0.047% at about 17–23 hour local siderial time. However, this fact must not be simply connected to the Compton-Getting's theory of galactic rotation, nor other anisotropies of cosmic rays outside the solar system. For, cosmic rays are deflected in the terrestrial and solar magnetic field, and the cosmic-ray diurnal variation suffer a disturbance attending to the solar or

geomagnetic activity.[4]

The analysis described above concerns to the averages for the whole periods of observations, which contain many disterved days. Now, it is desirable to examine on the quiet days only, to know the physical meaning above mentioned. Data at hand are insufficient for this purpose. However, we tried to examine the data obtained at Tokyo, to know the general tendency as a prelininary step.

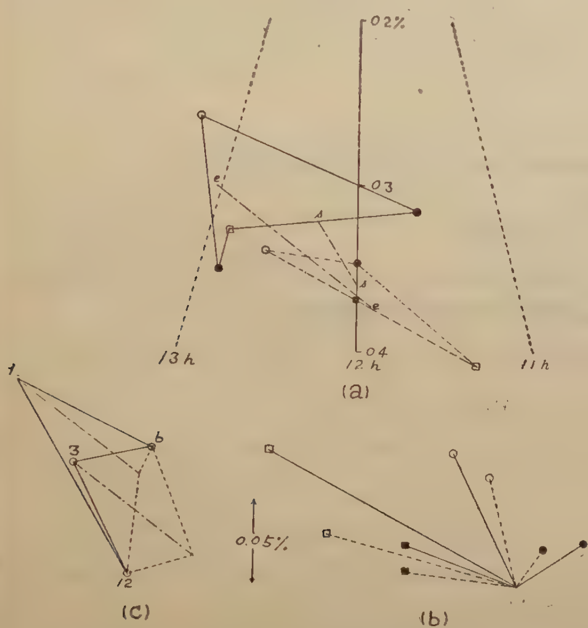

(a) (b) (c)

Fig. 6. Cosmic-ray diurnal variation in magnetically quiet days compared with that in the whole period.

In Fig. 6 (a), the dotted lines are the annual change at Tokyo, reproduced from Fig. 1, which contains the effect of disturbed days; while, the full lines are the result of similar treatment on the magnetically quiet days only. e and s are the averages for the spring-autumn and the summer-winter respectively.

As was expected from the nature of the disturbance in the cosmic-ray diurnal variation,[4] the diurnal variation of whole period has larger amplitude and advanced phase than those of quiet days, and the difference is larger in the case of e, which contains more disturbances, than in the case of s. Fig. 6 (b) shows difference vectors between quiet days and whole period in each season. Full lines were drawn from (a), where the quiet days are selected as the day n$\geq$4, n being the number of days after the commencement (n=o) of a magnetic storm. On the other hand, the dotted lines correspond to n$\geq$3. This result will mean that n$\geq$4 is not yet sufficient for the qualification of quiet days.

However, the difference e–s in Fig. 6 (a) may be worth attempting to know the tendency. If the world-wide annual change given in Fig. 5 (Y–Sj), which is reproduced as dotted line in Fig. 6 (c), is corrected for disturbance with e–s, thus obtaining the full line in (c), then it will represent something near the world-wide annual change in magnetically quiet days. In this result, the diurnal amplitude decreases and the phase retrocedes at equinoxes (3, 9). It may be possible that this result is explained with the fact that the angle between the earth's axis and orbit becomes small in the equinoxes, if the diurnal variation of cosmic-rays is attributed to a predominant flow of cosmic rays tangential to the earth's orbit. Such a flow is already suggested by Vallarta and Godart[5] and Alfven.[6]

For this research, monthly values of the harmonic coefficient of the diurnal

variation of barometer and temperature corrected cosmic-ray intensities at Canberra are communicated from Dr. Hogg, and hourly values of barometer corrected cosmic-ray intensities at Tokyo are supplied from the Nishina Laboratory of the Science Research Institute. The aerological data were supplied through the Central Meteorological Observatory, and the geomagnetic data were supplied through the Ionosphere Research Special Committee of Japan Science Council. This work was done upon the scientific research fund supplied from the Ministry of Education. The authors wish to express their cordial thanks to each of them. Thanks also due to Mr. T. Suzuki for his asistance in this work. (Aug. 10, 1950)

[1] A. Duperier, Sixieme Report Relations entre phenom. Solairs et Terr.
[2] A.R. Hogg, Nature, **162**, 613 (1948).
[3] B.F.J. Schonland, Terr. Mag. **42**, 137 (1937).
[4] Y. Sekido and S. Yoshida, Report of Ionosphere Research in Japan, **4**, 37 (1950).
[5] M.S. Vallarta and O. Godart, Rev. Mod. Phys. **11**, 181 (1939).
[6] H. Alfven, Phys. Rev. **75**, 1732 (1949).

Investigation of the Magnetic Storm by the Induction Magnetograph

By Yoshio KATO and Shinkichi UTASHIRO

Institute of Geophysics, Faculty of Science,
Tohoku University, Sendai

The authors observed $\frac{dH}{dt}$ of the earth's magnetic field of three compornents by the induction magnetometer at Onagawa ($\lambda=141°28'$E. $\varphi=38°26'$N) near Sendai and found following results.

At the time of sudden commencement of the first phase of the magnetic storm, the oscillation of $\frac{dH}{dt}$ is rather large, next in the interval till entering to the second phase the amplitude is small and after entering to the second phase the variation is very short and large amplitude continues distinctry.

Namely it can be said that in the first phase and the second phase of the magnetic storm, two kinds of radiant ray of different properties and of different velocity reached the upper atmosphere.

The type of the change $\frac{dH}{dt}$ at the sudden commencement varies respectively, according as it occurs in the night hemisphere or day hemisphere; that is the oscillation of $\frac{dH}{dt}$ is very remarkable at daytime, while it is very weak at night. In the day hemisphere the amplitude of the oscillation of $\frac{dH}{dt}$ is greater than that which occur in the night hemisphere. A remarkable micropulsation of $\frac{dH}{dt}$ at the sudden commencement frequently took places during the summer and equinox, while it is weak during the winter.

Above stated charactor is very remarkable and occures almost without exception. Figures show the records of sudden commencement of the magnetic storm by the induction magnetograph in the period of racent two years (1948 and 1949).

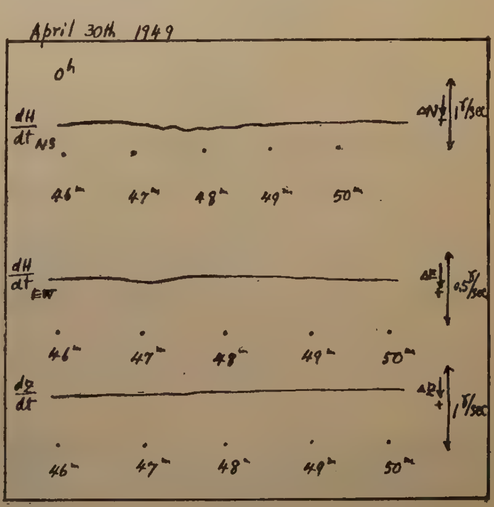

Fig. 1

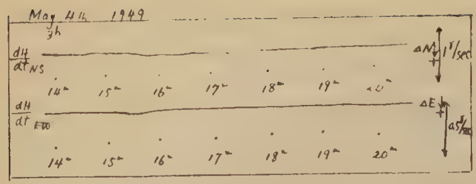

Fig. 2

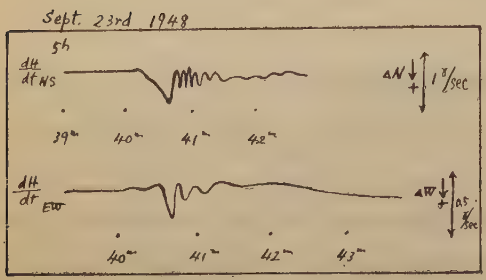

Fig. 3

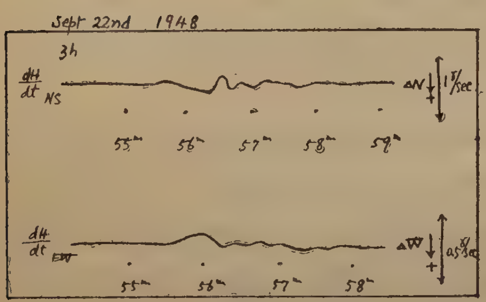

Fig. 4

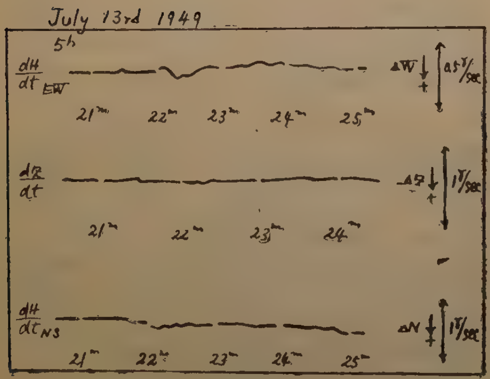

Fig. 5

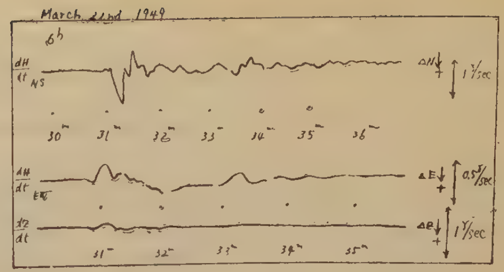

Fig. 6

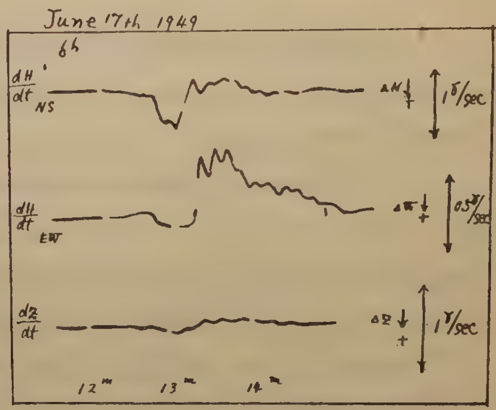

Fig. 7

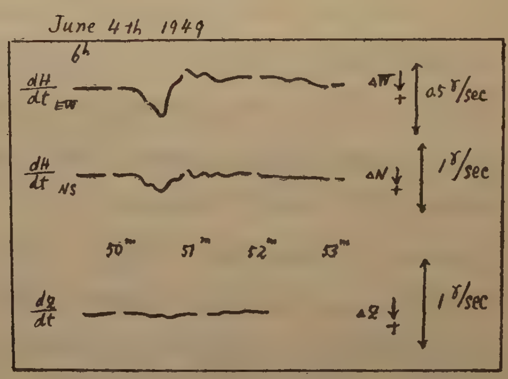

Fig. 8

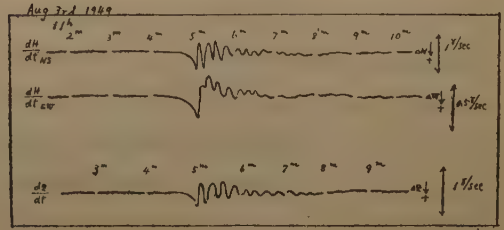

Fig. 9

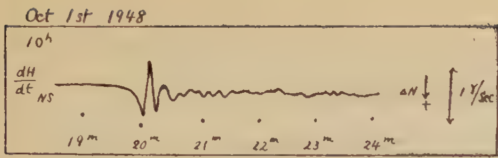

Fig. 10

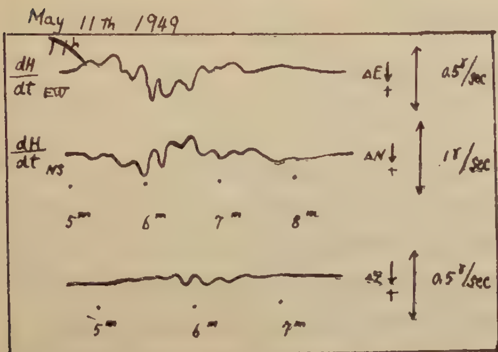

Fig. 11

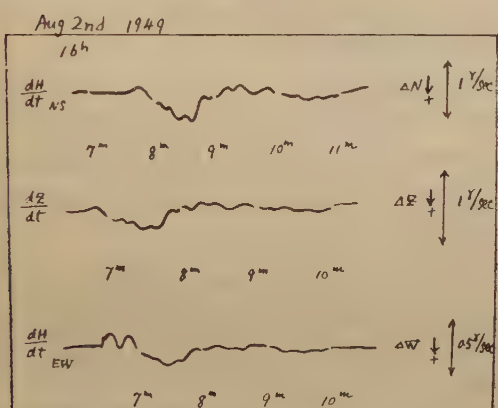

Fig. 12

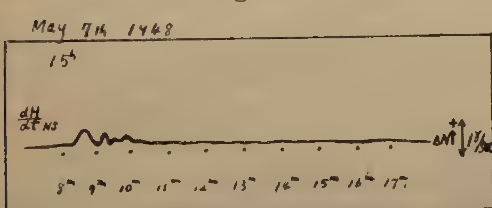

Fig. 13

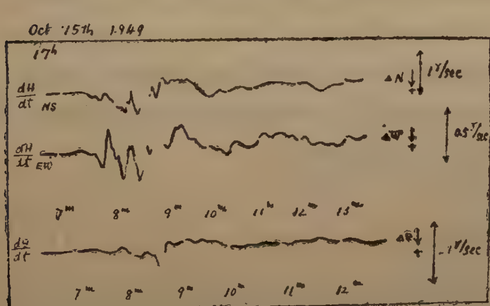

Fig. 14

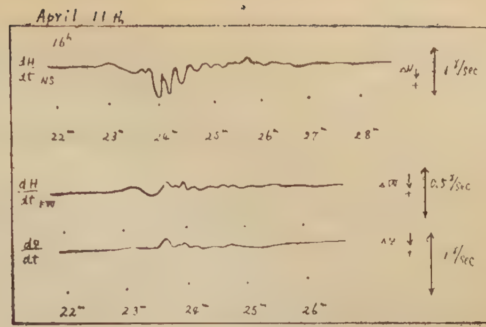

Fig. 15

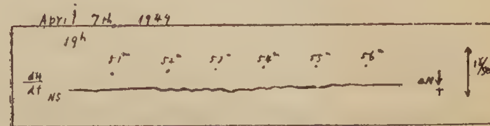

Fig. 16

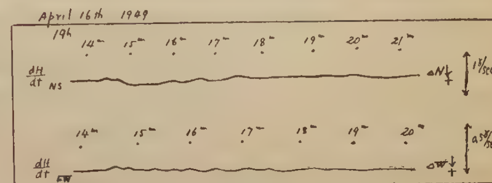

Fig. 17

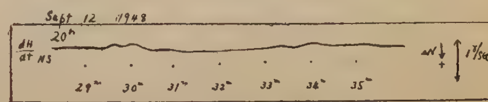

Fig. 18

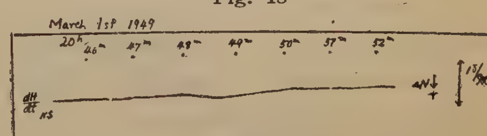

Fig. 19

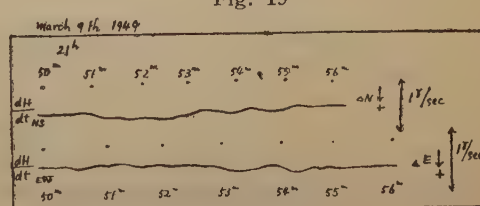

Fig. 20

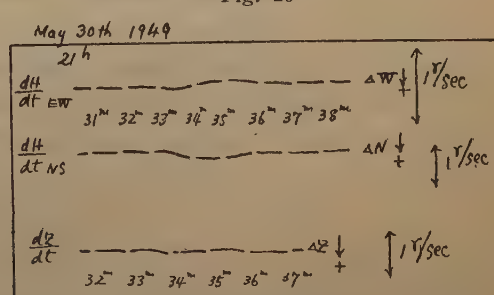

Fig. 21

On the Longitude Effect of a Corpuscular Stream from the Sun

By G. ISHIKAWA

Meteorological Research Institute

Many of the investigations hitherto made on the production of the ionosphere are based on the photo-ionization process and the results obtained seem to be valid for E-layer. There remain, however, many obscurities about the features of F-layer, of which the most essential concerns the diurnal variation of its electron density. The diurnal variation of the electron density in F-layer is so asymmetric that we ought to consider that it arises from an asymmetric distribution of incident ray. Such a possibility is hardly conceived so long as we adopt the photo-ionization process for the production of F-layer. But it may be considered likely if we visualize a charged particle in place of a photon as an ionizing source. A corpuscular stream coming in one direction from a place very distant from the earth will be affected by the earth's magnetic field so that the longitudinal distribution of incident particles near the earth should be asymmetric. The shape of such a distribution may be governed both by momentum and impact parameter of corpuscles.

Let us introduce rectangular coordinates x, y, z with origin at the earth's dipole (z-axis coincides with the magnetic axis) and assume that the direction of x-axis is in parallel with that of the motion of the stream at the long distance of L from the origin, where the field may be regarded as nearly equal to zero.

So that the initial state of a particle is given by the coordinates $s=(y)_{x=L}$ and $z_0=(z)_{x=L}$.

The equation of motion of a particle of mass m carrying a charge e is written as usual:

$$\dot{\boldsymbol{v}}=\frac{e}{m}(\boldsymbol{v}\times\boldsymbol{H}) \tag{1}$$

where $\boldsymbol{v}$ is the velocity of a particle and $\boldsymbol{H}$ is the magnetic field produced by a dipole of moment M. A perfect solution of this equation is not easily found, but numerical treatments are carried out by several authors. [1], [2], [3], [4] What is necessary here is not to find a perfect solution of trajectories, but to consider the general character of the possible solution. Making a transformation of variables from rectangular to polar coordinates r, θ, φ we obtain the solutions of equation (1):

$$\begin{aligned} r&=r\ (t,\ p,\ s,\ z_0)\\ \theta&=\theta\ (t,\ p,\ s,\ z_0)\\ \varphi&=\varphi\ (t,\ p,\ s,\ z_0)\end{aligned} \tag{2}$$

where p is the momentum of a corpuscle, which is conserved throughout the motion,

Then the position (θ, φ) of a particle of initial condition (p, s, z_0) at the earth's surface $(r=R)$ is readily obtained from the above solutions:

$$\theta=f_1\ (p,\ s,\ z_0)$$
$$\varphi=f_2\ (p,\ s,\ z_0) \tag{3}$$

So that the surface density σ of corpuscles at the earth's surface is given by:

$$\sigma\,(p,\ s,\ z_0)\,R^2 \sin\theta\, d\theta\, d\varphi=\sigma_0\, ds\, dz_0 \tag{4}$$

where σ_0 is the surface density of the stream of momentum p at $x=L$ plane. Eliminating s and z_0 from eqs. (3) and (4) we have:

$$\sigma\,(\theta,\ \varphi,\ p)=\sigma_0 f\,(\theta,\ \varphi,\ p) \tag{5}$$

This gives the longitudinal (together with the latitudinal) effect or the diurnal variation of incident intensity of a monochromatic corpuscular stream of momentum p.

If the stream has a momentum spectrum $\sigma_0(p)dp$ in the initial state, the required density distribution of the incident stream may be written as:

$$\sigma\,(\theta,\ \varphi)=\int_{p_0}^{\infty} \sigma_0(p)\, f(\theta,\varphi,p)\ dp \tag{6}$$

where the lower limit p_0 is the critical momentum with which the particle can reach the earth's surface from infinity.

The density distribution of incident particles at the earth's surface is thus governed both by a definite function $f\,(\theta,\varphi,p)$ and the momentum spectrum $\sigma_0(p)dp$.

Hence we may obtain a convenient distribution of σ for explaining the asymmetric and double maximal diurnal variation of F-layer, if we choose a suitable momentum spectrum in the corpuscular stream. The only points to examine are firstly whether such $\sigma_0(p)$ is likely or not and secondly whether the ionization by a corpuscle of such a momentum is enough to explain that actually observed in F-layer.

The treatment of the general case is not so easy and here we mention the special case of two dimentional problem in the equitorial plane. In this case we can readily obtain for the equation (3):

(A) for $s>-2C$

$$\varphi=\int_R^{\infty}\frac{(sr+C^2)dr}{r\,\{r^4-(sr+C^2)^2\}^{\frac{1}{2}}}\ , \tag{7}$$

where

$$C=\sqrt{eM/p} \tag{8}$$

is the well-known Störmer unit of length. The equation (7) is expressed in elliptic integral as usuals:

$$\varphi=\frac{\pi}{2}-\sin^{-1}(K\sin\psi)+\frac{s}{2\sqrt{2}\,C}F(K,\psi)\ , \tag{9}$$

where

$$K=\sqrt{4C^2+s^2}\ /2\sqrt{2}\,C\ , \tag{10}$$

$$\psi=\cos^{-1}\left\{-\frac{sr+2C^2}{r\sqrt{4C^2+s^2}}\right\}\ , \tag{11}$$

and $F(K, \psi)$ is the elliptic integral of the first kind.

(B) for $s < -2C$

$$\varphi = \frac{\pi}{2} - \psi - \frac{s}{\sqrt{4C^2+s^2}} F(K', \psi) , \tag{9$'$}$$

where

$$K' = \frac{2\sqrt{2}\,C}{\sqrt{4C^2+s^2}} , \tag{10$'$}$$

$$\psi = \sin^{-1}\sqrt{\frac{r^2-sr-C^2}{2r^2}} . \tag{11$'$}$$

For the equation (4) we have:

$$\sigma = \sigma_0 / R \left(\frac{\partial \varphi}{\partial s} \right)_{r=R} . \tag{12}$$

Using the equation (9) to (11), we obtain:

(A)

$$\frac{\partial \varphi}{\partial s} = \frac{4sC^2r^3 - s^4r^2 + 8C^4r^2 - 3s^3C^2r - 2s^2C^4}{r(16C^4 - s^4)\sqrt{r^4-(sr+C^2)^2}}$$
$$+ \frac{\sqrt{2}\,C}{4C^2+s^2} F(K, \psi) + \frac{2\sqrt{2}\,Cs^2}{16C^4-s^4} E(K, \psi) , \tag{13}$$

where $E(K, \psi)$ is the elliptic integral of the second kind.

(B)

$$\frac{\partial \varphi}{\partial s} = \frac{C^2[(s^4-16C^4)r^2 + 4s^2\{r^4-(sr+C^2)^2\}]}{r(sr+2C^2)(s^4-16C^4)\sqrt{r^4-(sr+C^2)^2}}$$
$$- \frac{1}{\sqrt{4C^2+s^2}} F(K', \psi) + \frac{s^2}{\sqrt{4C^2+s^2}(s^2-4C^2)} E(K', \psi) . \tag{13$'$}$$

The function $f(\varphi, p)$ is easily obtained using the eqs. (5), (12) and (13). Finally the lower limit p_0 in the equation (6) is given in this case by:

$$p_0 = \frac{eM}{(\sqrt{2}+1)^2 R^2} . \tag{14}$$

[1] C. Störmer: Zeits. für Astrophys. **1**, 237 (1930), Terr. Mag. **3**, 31 (1931).
[2] M.S. Vallarta: Univ. of Toronto Studies, Applied Math. Series. **3** (1938).
[3] M.S. Vallarta, C. Graef and S. Kusaka: Phys. Rev. **55**, 1 (1939).
[4] T. Yagi: Cosmic Ray Research, Nagoya Univ. III, **2**, 13 (1949).

Deflection of Cosmic Rays in the Solar Magnetic Field

By Yataro SEKIDO and Teiichiro YAGI

Physical Institute, Nagoya University

In order to investigate the sidereal-time variation of cosmic rays which may be connected with annual change of solar diurnal variation established by several authors recently, it is necessary to know the angles by which cosmic rays are deflected in the solar as well as the terrestrial magnetic field. Preliminary calculations in the equatorial plane will be reported here under the assumption that the sun's and the earth's dipole are parallel to each other.

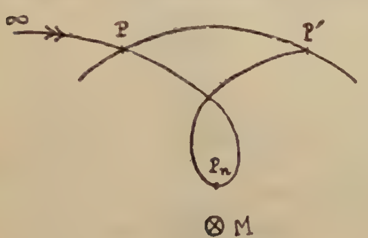

Fig. 1. Outer and inner orbit.

As seen in Fig. 1, particles in the same orbit may be observed at two points P and P', which are on a circle around the magnetic dipole M. The orbit ∞–P will be called as an outer orbit, while the orbit ∞–P–P_n–P' as an inner orbit, where P_n is the nearest point to the dipole M. When M is the earth's dipole M_e, and P, P' are on the earth's surface, it is unnecessary to consider the inner orbit, because it is absorbed by the earth's material. But, when M is the sun's dipole M_s, and P, P' are on the earth's orbit, it is necessary to treat also the inner orbit. The deflection angle in the outer orbit was already calculated by Vallarta et al.[1] An almost similar method can be applied (see remark) in the case of inner orbit. Result of our calculations about the inner orbit is shown in Fig. 2 with outer orbit together.

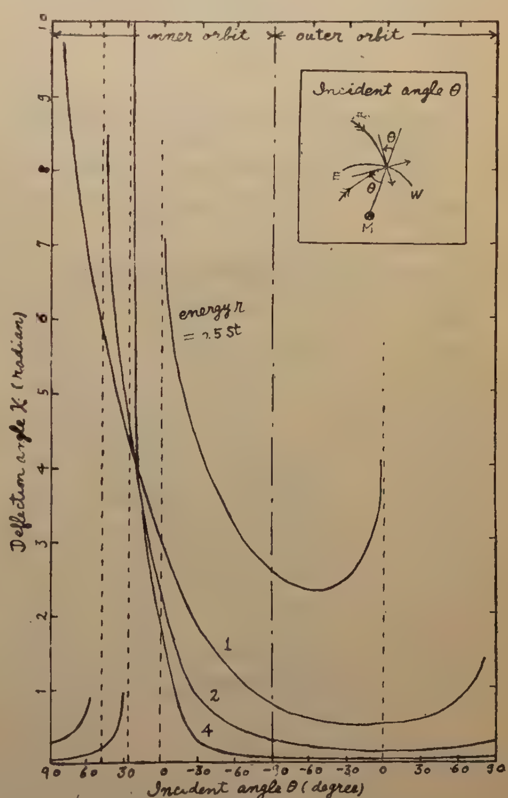

Fig. 2. Deflection angle χ of particles with incident angle θ. θ is counted positive eastwards for both outer and inner orbit. Broken lines correspond to asymptotic directions.

Next, deflection of cosmic rays passing through both the sun's and the earth's field will be treated.

Consider a boundary circle on which the sun's and the earth's field are equal to each other. Its radius is about fifty times as large as the earth's radius. Suppose that the sun's or the earth's

field predominates outside or inside this boundary circle. In Fig. 3 (a) the particle with energy r_e Störmer which incidents on the earth at a solar time t_e from a zenith angle θ_e travels in a direction of t' at the boundary circle.

Then, $$t' = t_e + \theta_e + \chi_e(r_e, \theta_e), \qquad (1)$$

where χ_e is the deflection angle of particle in the earth's field. Practically, the deflection angle when the radius of boundary circle is infinitely large may be adopted as χ_e. As the radius of boundary circle is negligible as compared with the distance between the sun and the earth, the particle which correspond to Fig. 3 (a) incidents

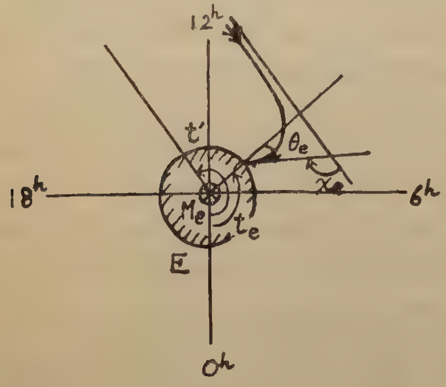

Fig. 3 (a). Deflection in the earth's field.

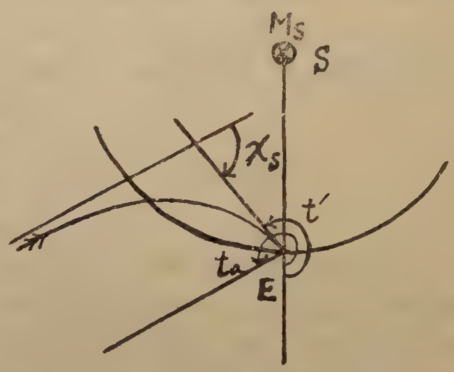

Fig. 3 (b). Deflection in the sun's field.

to a point E on the earth's orbit from the direction of t' in Fig. 3 (b). The initial direction t_a before it is deflected in the sun's field is

$$t_a = t' + \chi_s(r_s, t')$$
$$r_s = D/a_e \cdot (M_e/M_s)^{\frac{1}{2}} \qquad (2)$$

a_e: earth's radius D: distance between the sun and the earth.

From (1) and (2), the relation between t_e and t_a is known. Results in the case of $M_s = 10^{34}$ gauss. cm³ are shown in Fig. 4 (a), (b) and (c). As easily seen from the form of eq. (1) and (2), curves for a definit energy r_e and different directions θ_e are identical to each other except the translation along t_e axis.

As evident from Fig. 4, the deflections of particles with energy $0.5 \leq r_e \leq 1.0$ Störmer in the solar field are considerably large. Even if M_s is assumed to be $0.25 \cdot 10^{34}$ gauss. cm³ (0.43 is generally accepted as the mean value of M_s), the deflection of particles such that $r_e = 0.5$

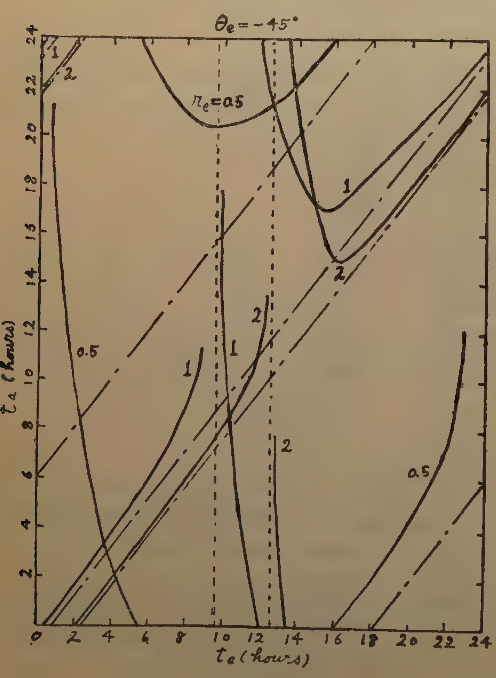

Fig. 4 (a)

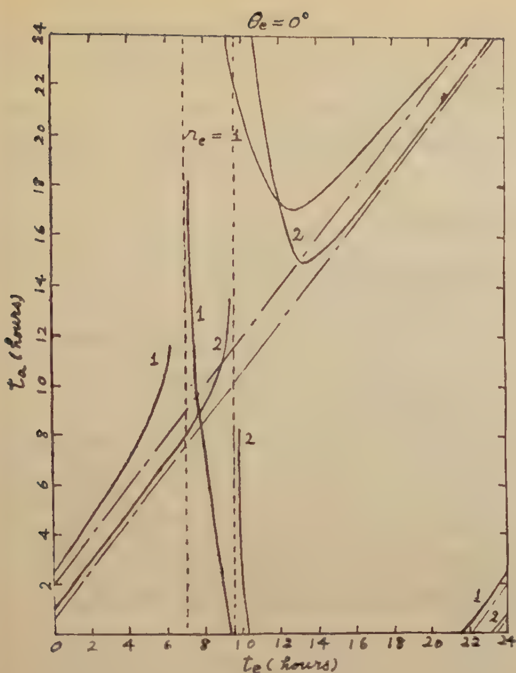

Fig. 4 (b)

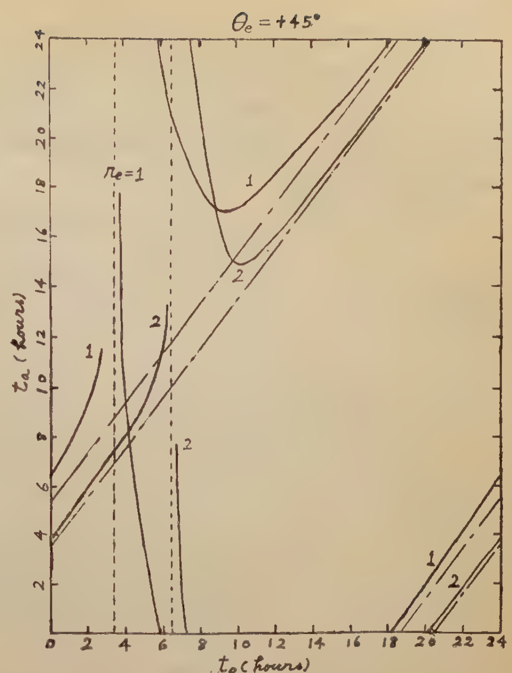

Fig. 4 (c)

Fig. 4. Relation between initial direction t_a and final incident time t_e. (t_a and t_e is expressed by solar time). (a), (b) and (c) correspond to those of incident directions of 45° west, vertical and 45° east respectively. —·—: case of earth's field only. ------: t_e which corresponds to asymptotic direction. r_e: energy in St. unit.

St. is still remarkable, for the curve of 0.5 St. is identical to that of 1.0 St. in the case of 10^{34} except a translation. Furthermore, the initial directions of the most particles which reach higher latitudes on the earth are near the equatorial plane. Therefore deflection in the solar field will be unable to be neglected in this case also.

In the calculation by Vallarta er al[(1)] about the sideral-time variation due to the galactic rotation, the effect of the solar field was not considered. If E^{-3} law is adopted as energy spectrum of primary cosmic rays, particles with energies almost near the cut-off energy only contribute to the sidereal time variation, as shown in the calculation by Vallarta et al. Thus, if the effect of solar field is taken into account according to Fig. 4, two maxima at least must be expected in the solar diurnal variation and their relative positions change with season, though the result will be more complicated if the inclination of the earth's dipole to the sun's one is taken into account.

[1] Vallarta, Graef and Kusaka, Phys. Rev. 55, 1 (1939).

Remark: Notations are the same as in reference 1.

Let polar coordinates, incident angle and deflection angle of particle be (r, ϕ), θ, and χ respectively.

Then $\qquad d\chi = d\phi \mp d\theta, \qquad -: r' < 0, \quad +: r' > 0,$

However, the following relations hold for the orbits in the equatorial plane: (1) $r'=0$ at the nearest point P_n only, (2) orbit is symmetrical with line $\overline{MP}_n$.

Thus, let the deflection angle for total, outer, and inner orbit be $\chi_{\text{tot.}}$, $\chi_{\text{out.}}$, and $\chi_{\text{inn.}}$ respectively, and let the longitude at infinity, P, and P_n be ϕ_a, ϕ_p and ϕ_n respectively, then

$$\chi_{\text{inn.}}=\chi_{\text{tot.}}-\chi_{\text{out.}}=2\left\{(\phi_n-\phi_a)-\left(\pm\frac{\pi}{2}\right)\right\}-\chi_{\text{out.}}$$

$$+:\ \gamma_1>1,\quad -:\ \gamma_1<1,$$

of course $$\chi_{\text{out.}}=(\phi_p-\phi_a)-\theta_p\,.$$

(Sept. 8, 1950)

On the Magnetic Moment of the Residual Magnetism of the Rock

By Yoshio KATO

Institute of Geophysics, Faculty of Science,
Tohoku University, Sendai

The author observed the magnetic susceptibility, the direction of the residual magnetism and the intensity of magnetization of many volcanic rocks collected from Izu-district.

The author investigated first the relation between the value of the susceptibility of the rock and amount of the magnetite in the sample.

The normative amounts of the magnetite in the sample used in this experiment are calculated from the data of the chemical analysis.

It is naturaly considered that the ferro-magnetic substance contained in the rock is magnetite, but we cannot know whether this magnetite exists in the state of pure crystal or a solid solution. If the magnetite exists in the state of pure crystal in the rock, we can calculate the apparent susceptibility of the rock itself, under the assumption that the magnetite is contained in the from of sphere. For example pumise of Mt. Komaga-dake, Hokkaido contains magnetite in the pure state, also the value of susceptibility is coincide absolutely to the calculated value. If the magnetite exists in the state of a solid solution in the rock, the value of susceptibility of the rock is less than the calculated value.

Fig. 1 shows the relation between the observed value of the susceptibility of

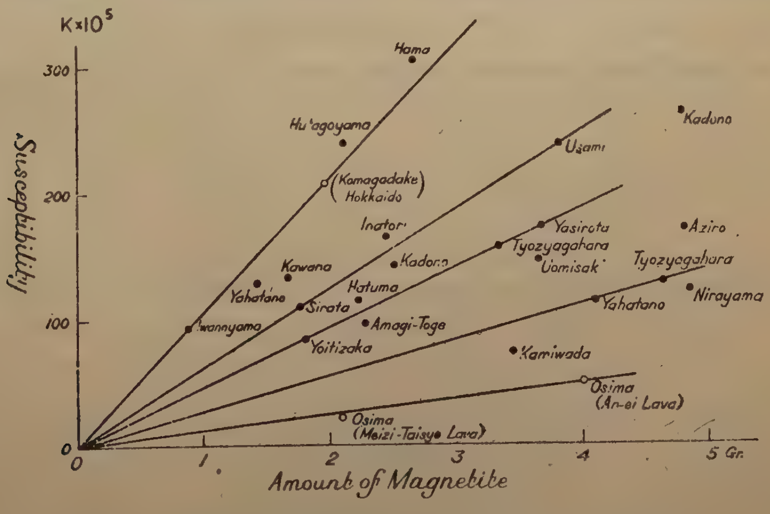

Fig. 1. Relation between the observed susceptibility and the amount of magnetite, contained in the rock.

the rock (which is given in the ordinate) and the normative amounts of the magnetite contained in that rock (given in the abscissa).

As the figure shows, the rocks of Komagadake, Iwanoyama, Futagoyama, and Hama form one strait line, while those of Sirata, Inatori and Usami form another strait line and so on.

It is concluded from these results, that the magnetite exists in the state of pure crystal in the rock of Komagadake, Iwanoyama, Futagoyama and Hama, and that the susceptibility of the rock depends on the amount of magnetite.

But in the rock of the Sirata, Inatori and Usami the magnetite exists in solid solution with other materials, and the value of susceptibility of these rocks depend on this magnetite in the state of a solid solution.

The susceptibility of a feromagnetic substance becomes less if it forms a solid solution with another paramagnetic substance, and it decreases its value gradually with the increasing of amounts of these para-or dia-magnetic substances.

Now next the author observed the direction of the parmanent magnetism and the intensity of magnetization of these rocks, and found that the intensity of magnetization of the rock increases its value when the magnetite contained in the rock exists in the state of solid solution.

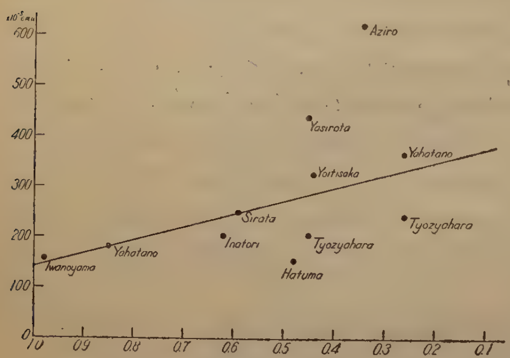

Fig. 2.

Fig. 2 shows the relation between the observed value of intensity of magnetization (which is given in ordinate) and the ratio of the observed value to the calculated value of susceptibility of the rock (which is given in the absissa).

As the figure shows the value of the intensity of magnetization becomes great if the ratio becomes small, that is the intensity of magnetization of the rock becomes great if the magnetite contains in the rock exists in the state of solid solution.

The KC type Magnetometer for Direct-vision
(Visually Recording Magnetometer)

By Tadao KUBOKI

Kakioka Magnetic Observatory

In order to use promptly the geomagnetic data in the ionosphere forcasting, it is desirable to record the geomagnetic variation in a light room where we can see the geomagnetic condition directly at any time. Some years ago, the writer constructed a magnetometer for direct-vision. Recently, he also succeeded in making continuous recording with higher accuracy.

The light beam which comes from the mirror of the variometer is reflected at the edges of two prismes, being separated into two rays which illuminate the respective photo-tubes. The photo-tubes are connected with an electric circuit in which the balance is kept when the tubes are illuminated equally. If it supposed that the balance is broken, the amplified electric current flows in the Helmholtz coil of which field deflects the magnet of the variometer so as to keep balance in the circut with the aid of negative feed back. This current changes proportionaly to the variation of the geomagnetism, and is recorded by a potentiometric recorder (single point).

The main characteristics of the magnetometer are as follows;

1. It is the continuous and visual record.
2. It is the remote recorder (we use one which the distance between recorder and magnetometer is 300 meters).
3. The scale-value is kept constant within the error of 1% at full scale (we called a-facter is very small), and does not change by the neverrness of the characteristics of the many electron tubes.
4. Corresponding to the fluctuation of 1 Volt in the power supply (100 Volts A.C.), the error amounts to 0.1–0.01%.
5. According to the use of the zero method we called the forged effect is very small.
6. The scale value on the recording paper is 0.5^{γ}–3^{γ}/mm.
   The variation of 50^{γ}–2000^{γ} can be recorded, and we can make these values to be variable by a same magnetic variometer.
   The natural period amounts to 0.4–1.5 seconds.

The magnetometer may be used also as X–, Y– or any component variometer by which the forged effects are exactly eliminated.

A highly sensitive magnetometer (scale value $2\times10^{-3}\,\gamma$/mm.) can be also constructed with the aid of positive feed back.

Example.

1. Scale value (observed value).

Date	Horizontal intensity	Declination
1950, Feb. 15	2.39 γ/div.	1.00 ′/div.
Apr. 18	2.45	0.99
Apr. 20	2.47	1.10
May 31	2.89*	0.735*
May 31	2.90	0.806*
June 14	2.88	1.05*
June 27	5.08*	1.06
July 11	5.10	1.11
July 22	5.02	1.03
Aug. 10	5.00	1.00
Sep. 4	5.04	1.01
Sep. 13	5.10	1.06
Sep. 28	5.08	0.94*
	(1 div. = 2.5 mm)	(1 div. = 3.0 mm)

* Changes by adjustment.

2. Base line value (observed value, no temperature-correction).

Date	Horizontal intensity	Date	Horizontal intensity
1950, Feb. 20	(30122) γ	1950, June 5	(30109) γ
Feb. 27	128	June 12	108
Mar. 6	130	June 26	—*
Mar. 7	130	July 4	150
Mar. 13	130	July 10	157
Mar. 14	126	July 14	163
Mar. 20	120	July 17	172
Mar. 27	120	July 25	176
Apr. 3	120	July 31	173
Apr. 10	114	Aug. 7	176
Apr. 17	118	Aug. 14	172
Apr. 24	117	Aug. 24	177
May 1	115	Aug. 28	173
May 4	118	Sep. 4	174
May 8	119	Sep. 11	177
May 15	115	Sep. 19	181
May 25	112	Sep. 25	174
May 29	114	Oct. 3	175
May 30	108	Oct. 9	172

* Changes by adjustment.

The temperature inside the variation room was 5°–7°C in February, 21°–24°C in June and 19°–15°C in October

The temperature-coefficient of variometer was adjusted to be 0.3 γ–0.5 γ/°C by means of the shunt alloys Fe–Ni–Cr system.

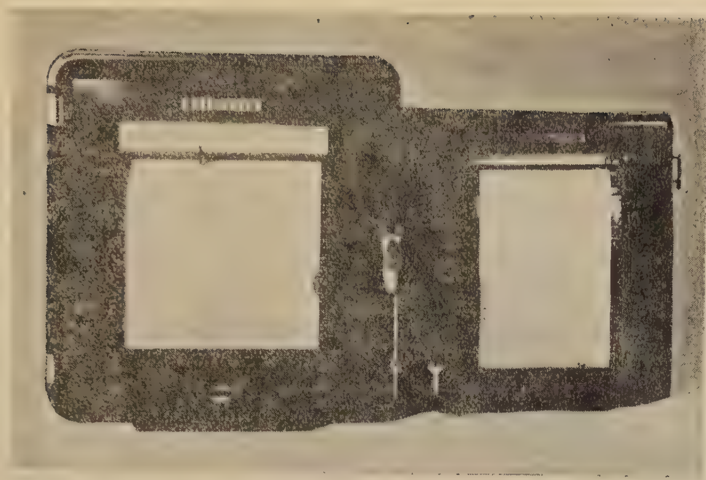

Fig. 1. Recorder (right H, left D)

Fig. 2. The KC type Magnetometer for Direct-vision Idiv. = 2.39γ (Horizontal intensity)

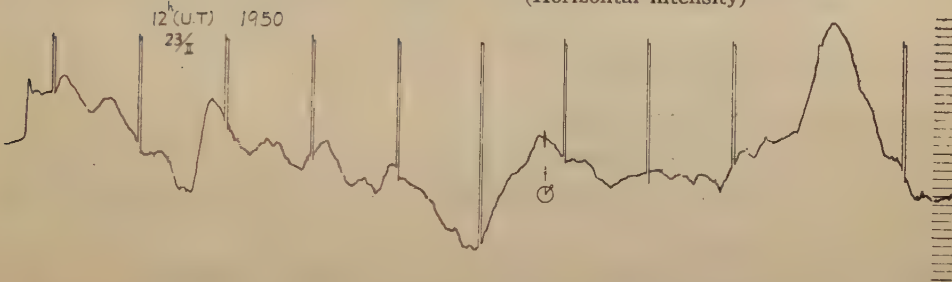

Fig. 3. The KC type Magnetometor for Direct-vision Idiv. = 0.985′ (Declination)

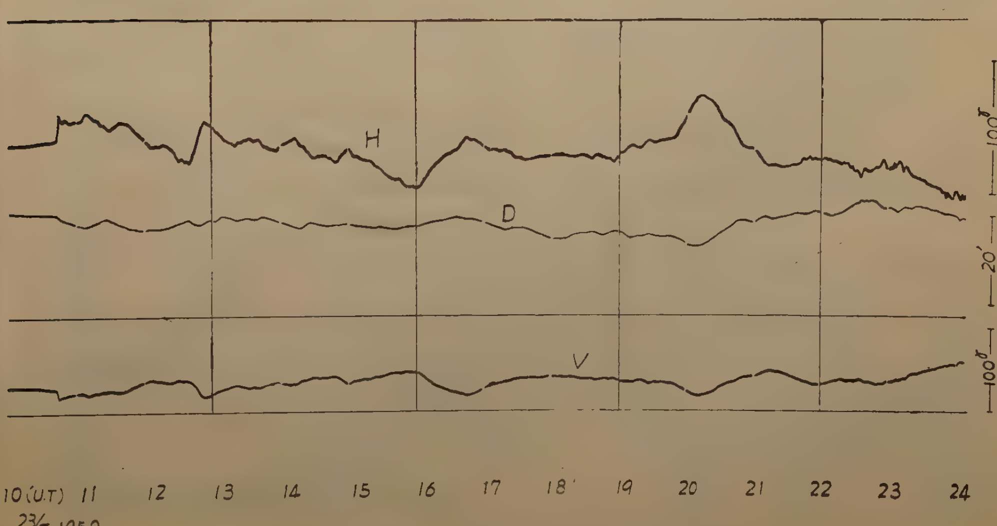

Fig. 4. Ordinary Variometer

Geomagnetic Activity Characterized by the K Indices

By Masaziro OTA

Aso Magnetic Observatory, Kyôto University

§ 1 Introduction

Statistical investigations of the geomagnetic activity can be carried out by utilization of the K Indices. Diurnal variation of the K Indices are dicussed by J. Bartels on his first paper(1) and percentage of K_H indices amended to K_D and K_V are researched by J. Crichton.(2) Recently, Bartels introduced the standard indices and the planetary indices as supplement of the ordinary K Indices.(3) The writer will discuss the diurnal variations of the magnetic activity and the nature of magnetic disturbances in view of the K Indices.

§ 2 Diurnal variation of the K variation

Figs. 1 and 2 show diurnal variations of the K Indices arranged concerning the local time at various observatories from the auroral zone to the equator, Fig. 1 was

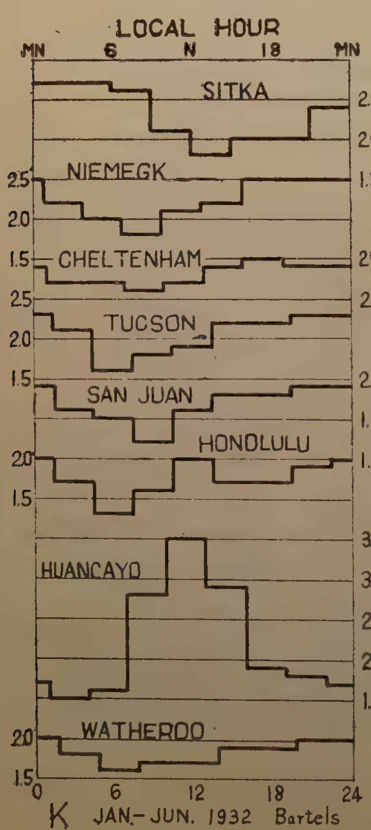

Fig. 1

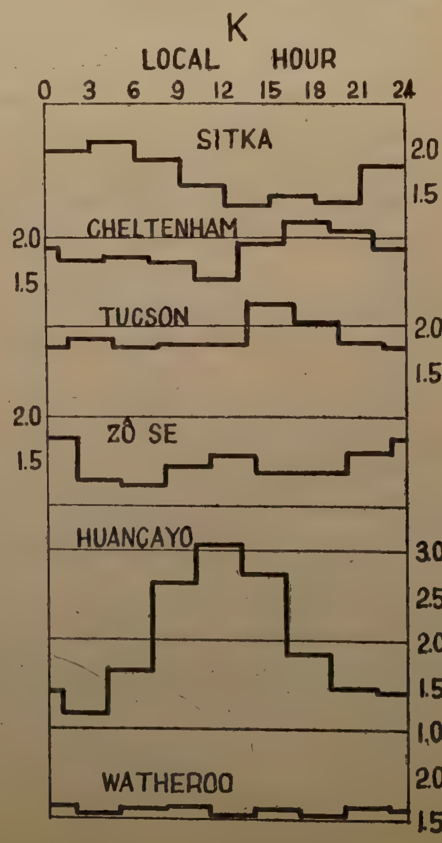

Fig. 2

given by Bartels and Fig. 2 was computed by the writer. In these figures we can see the noon-maximum of K values at the stations situated on the middle latitude such as Honolulu and Zô Sè. On this point Bartels says that there is a "hybrid between the types shown for Huancayo and San Juan", but the writer should rather like to explain that this is caused by the shift of the Sq current-system which occurs day by day along the meridian, because the curve of diurnal variation of H-component changes its type day to day at the observatories situated near the center of the vortex of the Sq current-system, and it makes increase K values near the noon.

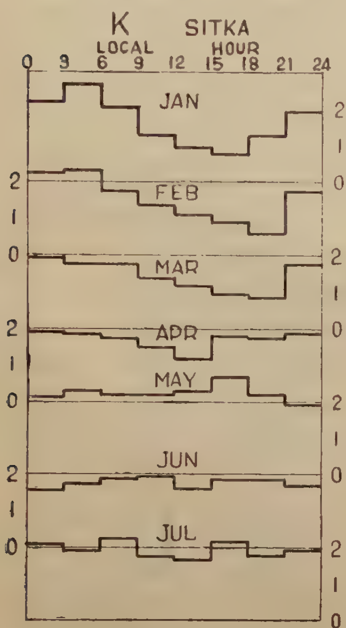

Fig. 3

At the still higher latitude from this region, it is recognized that the another maximum occurs on the evening. Judging from the Chapman's S_D-current-system it may be considered that this evening-maximum denotes the S_D-variation, and this amount will be taken as a measure to estimate an activity of the S_D-field at the middle latitude.

Fig. 3 shows monthly means of diurnal variations of the K Indices at Sitka. In this figure we can see that a type of diurnal variation of the K Indices has seasonal change. In winter months the night-disturbance predominates, this phenomenon is often seen at the Polar Region and it may be considered that this is the polar type of diurnal variation of the K. On the contrary, in summer months the values of the K Indices are large on the evening.

In the present case, we cannot have any conclusion respect to a day-to-day's activity of the S_D-field, the above discussion is only referable to the average state of one month or more.

For the purpose of a study of daily activity of the terrestrial magnetism, the nature of K variation (K_2 variation, after Bartels) must be also introduced as well as the ranges of the variation. As for the S_D-field at the middle and lower latitudes, statistical investigations are not so complete as those at the auroral zone. It is desirable that the diurnal variation of the K Indices is responsible for the study of S_D, especially evening-maximum of K is thought to express the S_D-activity. Moreover, it is also desirable that the time of evening-maximum and the shape of the H-curve are to be shown by another character-figure.

§ 3 Frequency-distribution of K values at different observatories about the same E-time

It is desirable that K values of every E-time have the same values at the all observatories, the writer will consider about this point in this paragraph. Fig. 4 shows the frequency-distribution of K values about the E-time at which the K_w is less than 0.4. In this figure the frequency of K=0 predomintes compared with K=1,

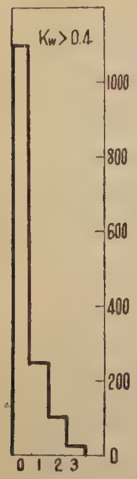

Fig. 4

2 or 3, and the value larger than 4 do not exist at any station. Then, it may be said that the K Indices satisfy its original property during the quiet time. Next, the writer tried the same treatment about the E-time when the K_w is larger than 5, and are shown in Fig. 5. Fig. 6 shows the frequency-distribution of deviations of K values from their means of the all observatories at every E-time during the large storm (Mar. 12—15, 1948). From these two figures it can be seen that the frequency-distribution is spreaded very widely, especially the neighbouring values of the maximum frequency have almost same numbers. If the limits of K Indices are classified according to the original definition, this distribution is to have a sharp maximum, but this condition is not satisfied at the E-time when the K Indices have large values, that is to say, the original condition of K is not satisfied during disturbance-times.

The natures of disturbances will make to take different K-values at the various observatories, then it is difficult to take the same value about all stations, so far as a single index is used. To satisfy this condition, the limits of K values are taken such that it is not only a function of the geomagnetic latitude but also a function of the geomagnetic longitude, because the auroral zone is not a complete circle and the line of the magnetic equator suitable for the K Indices is not clear so far as concerning the distribution of the observatories.

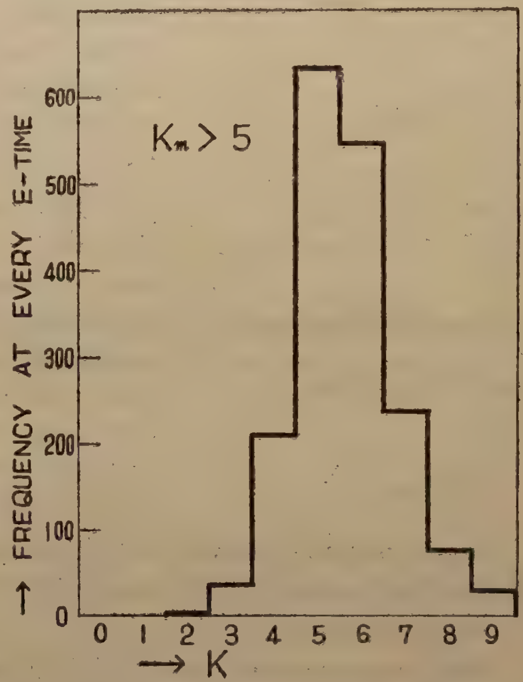

Fig. 5

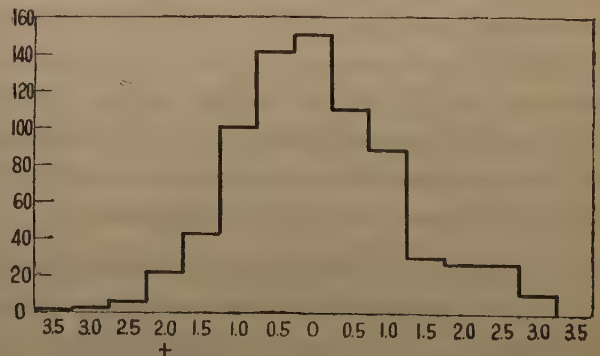

Fig. 6

[1] Terr. Mag. 44, 447 (1939).

[2] Jour. Geophy. Res. 54, 275 (1949).

[3] Table of the K Indices, (1948).

Magnetic Survey in Japan

Geographic Survey Institute

Since 1949, first order magnetic survey in Japan had been carried out by the Geographic Survey Institute. In 1949, 10 stations were surveyed in the southwestern part of Japan, and in 1950, 30 stations in northwestern part. 30 stations will be added in the southwestern part in 1950. Furthermore, about 15 stations will be selected for the magnetic standard points from these first order magnetic points, for the purpose of studying on secular variations of the geomagnetic elements and of correct mapping of the magnetic chart.

(1) First order magnetic survey.

The stations are distributed uniformly and amount 70 points in Japan. The mean distance between them is about 60 km. Since they are marked by the monuments made of granite, it is possible to reoccupy the strictly same points in future. In ordinary, they will be resurveyed every five years.

(2) Standard magnetic station.

From the first order magnetic points, standard magnetic stations are selected by the following conditions.

1. Local magnetic anomaly is small as possible.
2. They are free from artificial magnetic disturbances even in future.
3. The distance between each station is about 120 km., and their distribution is as uniform as possible in Japan.

These stations will be reoccupied every other year.

(3) Instruments.

The instrument used for these surveys is GSI type magnetometer. This is the one of the induction type magnetometer, and can measure the three elements of geomagnetic field almost simultaneously with the accuracy of 0.′1 in declination and dip, and 1 γ in intensity.

(4) Result of the survey in 1949.

The measurement of three elements were carried out every hour through 26 hours at each station, except the day of magnetic storm. Each result was reduced to the epoch 1950. The reduced values are shown in Table 1.

Here, altitude corrections were neglected, no station being so high.

From these reduced values, the empirical equations of quadratic form for the three elements were derived by the method of least squares. The calculated equations are as follow;

$$D = -6°17.2' + 0.4577\Delta\varphi - 0.0690\Delta\lambda - 0.00536\Delta\varphi^2 - 0.00035\Delta\lambda^2 - 0.000586\Delta\varphi\Delta\lambda,$$

$$I = 48°46.1' + 1.2787\Delta\varphi - 0.1816\Delta\lambda - 0.000137\Delta\varphi^2 + 0.000145\Delta\lambda^2 - 0.000748\Delta\varphi\Delta\lambda,$$

$$H = 30922 - 6.46408\Delta\varphi - 1.30995\Delta\lambda - 0.00349\Delta\varphi^2 - 0.00153\Delta\lambda^2 + 0.00674\Delta\varphi\Delta\lambda.$$

Where, φ and λ stand for the north latitude and the east longitude and $\Delta\varphi=\varphi-35^\circ$ $\Delta\lambda=\lambda-135^\circ$ expressed in minutes of angle.

The curves drawn by these equations are shown in Figs. 1, 2, and 3.

Table 1

Station	Longitude	Latitude	Reduced value (obs.)	Calculated value
Kanoya	130°52.9′E	31°25.2′N	D -4°48.6′ I 44 33.0 H 32725	-4°47.0′ 44 31.2 32738
Fukuoka	130 22.1	33 32.6	D -5 40.1 I 47 36.1 H 31901	-5 43.2 47 39.1 31867
Tenjinno	133 48.0	35 25.0	D -6 42.5 I 49 43.2 H 30746	-6 34.8 49 33.4 30833
Kawanoe	133 33.8	34 0.1	D -5 54.8 I 47 40.6 H 31441	-5 54.2 47 42.7 31434
Imazu	135 59.5	35 21.1	D -6 21.4 I 48 58.8 H 30740	-6 22.0 49 1.7 30709
Hamamatsu	137 41.3	34 44.6	D -6 0.0 I 48 2.9 H 30753	-5 59.7 48 3.2 30752
Himi	136 55.5	36 52.1	D -6 54.9 I 50 37.0 H 30118	-6 59.1 50 42.4 30070
Shibata	139 16.5	37 58.1	D -7 13.3 I 51 39.6 H 29339	—— ——
Katsuura	140 18.0	35 12.9	D -5 54.9 I 48 14.4 H 30315	-5 54.8 48 16.1 30294
Shingu	136 0.0	33 43.8	D -5 40.7 I 47 2.7 H 31282	-5 43.9 47 2.8 31279
Kakioka (Observatory)	140 11.0	36 14.0	D -6 18.0 I 49 27.0 H 29980	-6 15.1 49 21.4 30024

INCLINATION
FOR 1950

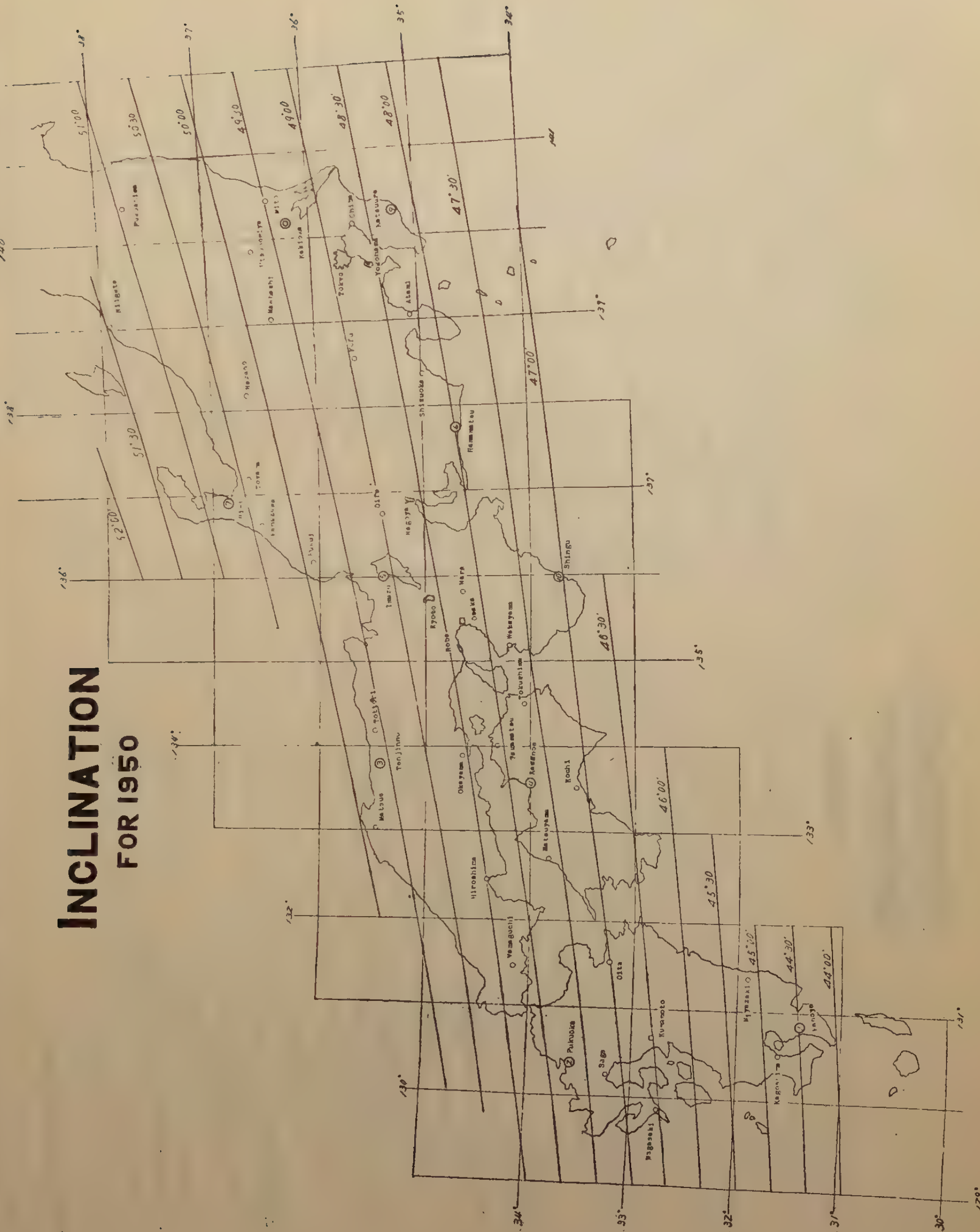

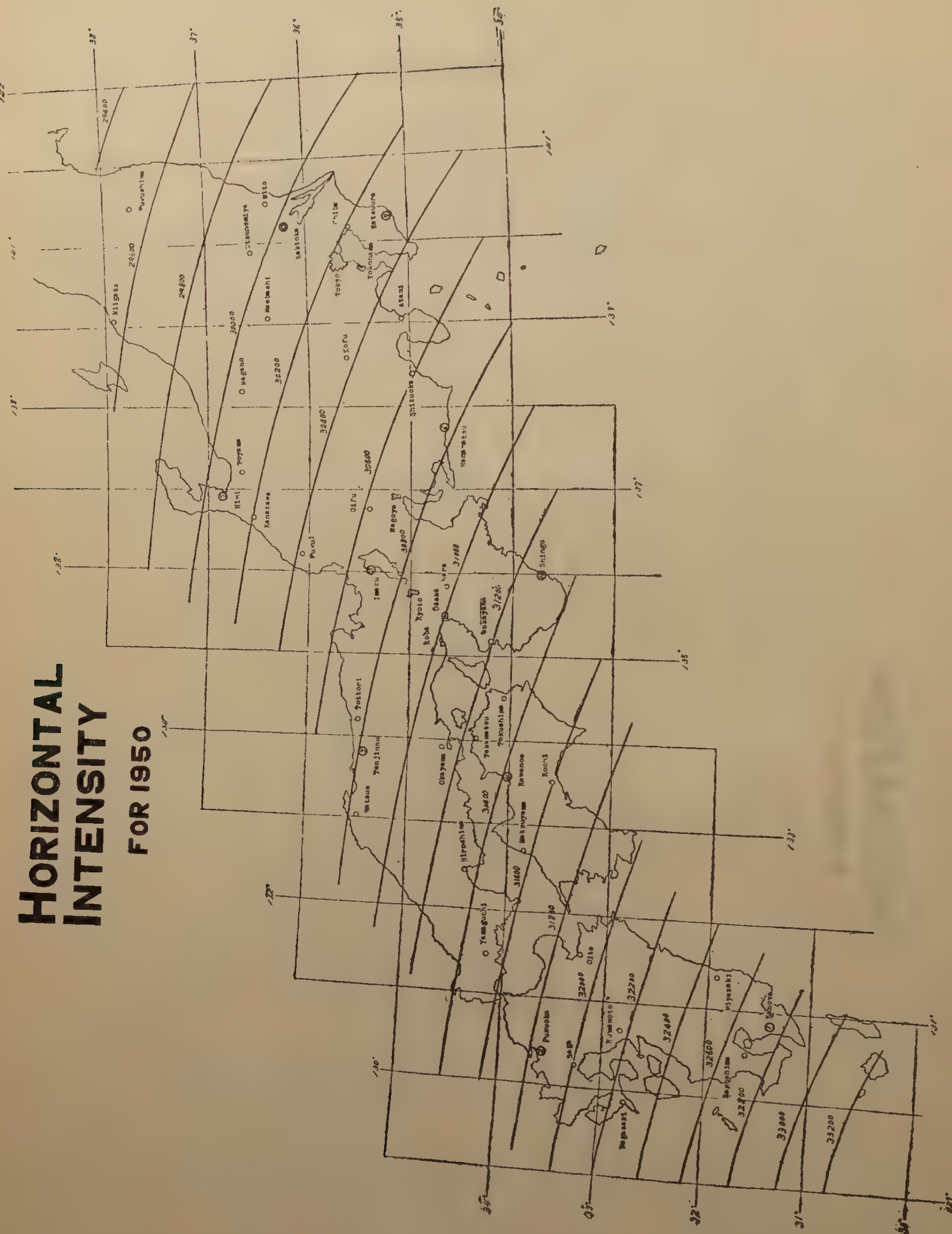

HORIZONTAL INTENSITY FOR 1950

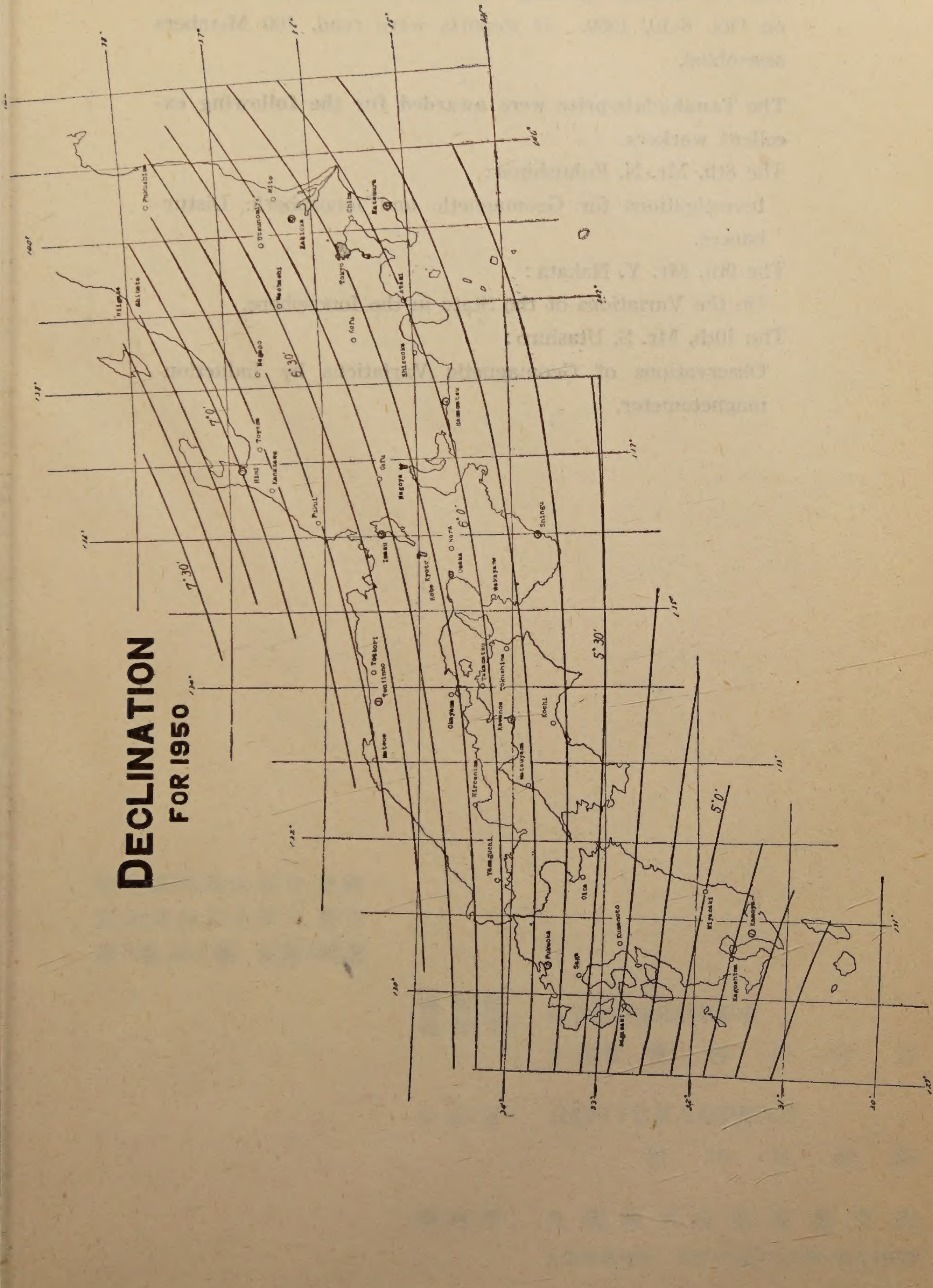
DECLINATION
FOR 1950
7°30'
7°0'
6°30'
6°0'
5°30'
5°0'

The Meeting of the Society of Terrestrial Magnetism and Electricity.

The 8th General Meeting. Held at the Tohoku University on Oct. 8–10, 1950. 54 Reports were read, 100 Members assembled.

The Tanakadate-prize were awarded for the following excellent workers.

The 8th, Mr. N. Fukushima:

Investigations for Geomagnetic and Ionospheric Disturbances.

The 9th, Mr. Y. Nakata:

On the Variations of the State in the Ionosphere.

The 10th, Mr. S. Utashiro:

Observations of Geomagnetic Variations by Induction-magnetometer.

昭和25年12月25日 印刷
昭和25年12月31日 發行
第2巻 第3號　定價150圓

編輯兼發行者　日本地球電氣磁氣學會
代表者　長　谷　川　万　吉

印刷者　京都市下京區上鳥羽學校前
田　中　幾　治　郎

賣捌所　丸善株式會社京都支店
丸善株式會社　東京・大阪・名古屋・仙台・福岡

JOURNAL OF GEOMAGNETISM AND GEOELECTRICITY

Vol. II No. 3

1950

CONTENTS